Journal of Power Sources 193 (2009) 593–597

Contents lists available at ScienceDirect

Journal of Power Sources

journal homepage: www.elsevier.com/locate/jpowsour

Short communication

Fe doping effects on phase stability and conductivity of $La_{0.75}Sr_{0.25}Ga_{0.8}Mg_{0.2}O_{3-\delta}$

Jin Seong Yoo[a], Shiwoo Lee[b,*], Ji Haeng Yu[b], Sang Kuk Woo[b], Hun Park[a], Ho Gi Kim[a]

[a] Department of Materials Science and Engineering, KAIST, Daejeon, 305-701, Republic of Korea
[b] Energy Materials Research Center, Korea Institute of Energy Research, Daejeon, 305-343, Republic of Korea

ARTICLE INFO

Article history:
Received 25 March 2009
Accepted 15 April 2009
Available online 23 April 2009

Keywords:
LSGM
Solid oxide fuel cells
Solid electrolyte
Transition metal
Ionic conductivity
Neutron diffraction

ABSTRACT

The effects of Fe doping on phase stability and electrical conductivity were investigated for the 25 mol% Sr and 20 mol% Mg-doped lanthanum gallates (LSGM-2520). While secondary phases, in addition to perovskite phase, were formed for an undoped LSGM-2520 in accordance with previous reports, a single phase perovskite phase was obtained by addition of a small amount (~4 mol%) of Fe to LSGM-2520. The conductivity of 4 mol% Fe-doped LSGM-2520 was as high as 0.17 S cm^{-1} at 800 °C and it was confirmed to be ionic based on its dependency on oxygen partial pressures. Crystallographic analysis using neutron diffraction and electron diffraction determined the crystal structure and lattice parameters for 4 mol% Fe-doped LSGM-2520.

1. Introduction

Sr- and Mg-doped $LaGaO_3$-based perovskite (LSGM) is a promising solid electrolyte for solid oxide fuel cells (SOFCs) which can be used at lower temperatures compared to conventional fuel cells based on yttria-stabilized zirconia [1,2]. Various research groups have recognized the high oxide ion conductivity of LSGM and demonstrated its high power density by combining LSGM with relevant electrode materials [3,4].

The oxide ion conductivity of $LaGaO_3$-based solid electrolyte is strongly dependent on the amount of Sr^{2+} and Mg^{2+}, because both ions substituting La^{3+} and Ga^{3+}, respectively, produce oxygen vacancies in the host lattice. An increase in the conductivity of $LaGaO_3$ to a certain level with an increase in Sr^{2+} and Mg^{2+} doping indicates that oxygen vacancies contribute to oxygen ion conduction. The solubility limit of one dopant in $LaGaO_3$ is also a function of the amount of the other one. For example, while the solid solution range of $La_{1-x}Sr_xGaO_{3-\delta}$ was limited to $x = 0.1$, more Sr^{2+} could be soluble when Mg^{2+} was substituted for Ga^{3+} ions [5]. It has been generally known that solubility limits of both Sr and Mg in $LaGaO_3$ to form highly ionic conductive phase are around 0.2, and this region shrinks with decreasing temperature [5–7]. Excess addition of dopants over the limits may produce significant amount of oxygen vacancies but also can cause a vacancy ordering, which is deleterious to transport of oxide ions [8].

The results of the study reported here suggest that the solubility limit of Sr^{2+} can be expanded by a substitution of a transition metal for the B-site cations. Doping of transition metals is not a new strategy, especially in the $LaGaO_3$ system. It has been reported that the oxide ion conductivity of LSGM increased by doping small amount of transition metal, such as cobalt [6,7] and iron [8,9], without decreasing the transport number of the oxide ions. For example, Ishihara et al. found that cells using Co-doped LSGM as an electrolyte exhibited a notably higher power density [10]. However, all the compositions studied were the ones which had 20 mol% or less in Sr doping level and there was no report on how transition metal doping affects an electrolytic domain in a compositional aspect. As the doping of transition metal in B-sites causes a change in structural parameters of the lattice, stable compositional range of A-sites cations will be varied concurrently. Therefore understanding of the doping effect on crystallographic structure and electrical property enables us to discover new electrolyte compositions. In the present study, we discuss the phase stability and conductivity of Fe-doped LSGM with a "Sr-rich" composition (25 mol%), or $La_{0.75}Sr_{0.25}Ga_{0.8}Mg_{0.2-x}Fe_xO_{3-\delta}$ ($x = 0$–0.08) and report the results of a crystallographic analysis for a promising electrolyte composition.

2. Experimental

The $La_{0.75}Sr_{0.25}Ga_{0.8}Mg_{0.2-x}Fe_xO_{3-\delta}$ ($x = 0$–0.08) samples were synthesized from the following materials: La_2O_3 (99.99%, Aldrich Chemical; the rest are the same), $SrCO_3$ (99.9%), Ga_2O_3 (99.99%), MgO (99.9%), and Fe_2O_3 (99.9%). The stoichiometric amounts of raw

* Corresponding author. Tel.: +1 215 898 0056; fax: +1 215 573 2093.
E-mail address: shiwoo@seas.upenn.edu (S. Lee).

0378-7753/$ – see front matter © 2009 Elsevier B.V. All rights reserved.
doi:10.1016/j.jpowsour.2009.04.025

powders were ball-milled with isopropyl alcohol for 24 h and dried. The mixture was then calcined at 1523 K for 2 h in air and crushed in an agate mortar. The resulting sieved powders were sintered at 1773 K for 5 h in air.

The calcined powders were examined by high resolution X-ray diffraction (XRD, Rigaku) using Cu Kα radiation. Thermogravimetric analysis (TGA, TA instruments) for each powder composition was conducted with increasing temperature. For this analysis, the sintered powders were first annealed at 1073 K for 2 h in air and quenched to room temperature. While heating with a rate of 5 K min^{-1}, the weight losses of the samples were measured under a high purity nitrogen flow of 90 ml min^{-1}. The electrical conductivities of the samples were measured using a 4-probe D.C. method while changing temperatures and oxygen partial pressure by adjusting the relative amount of H_2/H_2O or CO/CO_2. Oxygen partial pressures were measured using a zirconia oxygen sensor.

The neutron diffraction data was obtained at the wavelength of 1.8356 Å on a high resolution powder diffraction (HRPD) beam line at the Korea Atomic Energy Research Institute. Experimental conditions were as follows: monochrometer: Ge(3 3 1): take-off angle ($2\theta_M$), 90°; collimators: 6′, 10′, 20–30–10′; detector: 32 ^{3}He detectors (5° apart); 2θ range: 10–159.95°; sample can: vanadium. The structural analysis from neutron diffraction data was performed via Rietveld refinement method using the Fullprof^{TM} program. The microstructures were analyzed using a transmission electron microscope (TEM, Tecnai 30 S-Twin) operated at 300 kV. TEM samples were prepared by dispersing in ethanol and then dropping on a carbon coated copper grid.

Throughout the paper, the composition, $La_{0.75}Sr_{0.25}Ga_{0.8}Mg_{0.2-x}Fe_xO_{3-\delta}$, is referred to as LSGMF. Numbers following the abbreviation correspond to the mole fraction of Sr, Mg and Fe in each site of ABO_3 perovskite. For example, $La_{0.75}Sr_{0.25}Ga_{0.8}Mg_{0.16}Fe_{0.04}O_{3-\delta}$ is designated as LSGMF-251604.

3. Results and discussion

3.1. Fe doping effect on phase stability, mass and conductivity

Phase stability: Fig. 1(a) shows high resolution XRD patterns of LSGM-2520, LSGMF-251802, LSGMF-251604, and LSGMF-251208. Bars at the position of the $LaGaO_3$ perovskite phase are presented for reference. Fig. 1(b) shows that the peak corresponding to the (1 1 0) plane is shifted toward higher 2θ as Fe substitution is increased, which indicates that some of the Mg^{2+} ions (ionic radius = 66 pm) with 6-fold coordination were substituted by smaller Fe^{3+} ions (~64 pm).

Diffraction peaks of the secondary phases identified as $LaSrGaO_4$ (JCPDS 24-1208) and $LaSrGa_3O_7$ (JPCPS 45-0637) were observed in the pattern of LSGM-2520 (Fig. 1(a)), which supports the previous report that the solubility limit of Sr in $LaGaO_3$ is around 20 mol% when mole fraction of Mg was fixed to 20 mol% [5,11]. Recently, Li et al. also reported that 25 mol% Sr-containing LSGM showed low stability of the perovskite phase and lots of secondary phases [12].

On the other hand, the peak intensity of the secondary phases decreased noticeably in the pattern of 2 mol% Fe-doped LSGM (LSGMF-251802) and especially the peaks corresponding to $LaSrGa_3O_7$ were hardly detected. Furthermore, for 4 mol% Fe-doped LSGM (LSGMF-251604), peaks for all the secondary phases including those for $LaSrGa_3O_7$ disappeared. It is evident that Fe ions, the substitute for Mg ions, have a structurally stabilizing effect on LSGM which has a Sr^{2+} composition higher than 20 mol%, or solubility limit. Interestingly, by adding more Fe in the place of Mg, secondary phase peaks were observed again, even though they were not significant in intensity. Consequently, the compositional range of Fe substitution for Mg in LSGM-2520 systems to maintain primary perovskite phase with high symmetry are estimated to be less than 8 mol% of B-site cations.

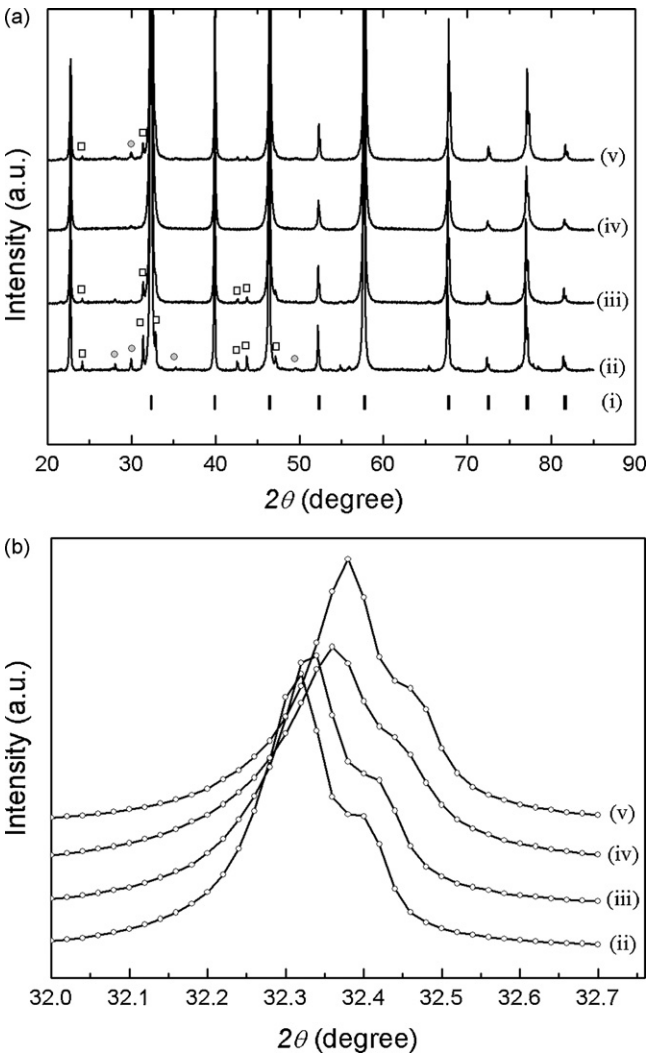

Fig. 1. XRD patterns of $La_{0.75}Sr_{0.25}Ga_{0.8}Mg_{0.2-x}Fe_xO_{3-\delta}$ measured at room temperature: (a) at the range of 2θ = 20–85° and (b) 2θ = 32–32.7° for (i) $LaGaO_3$, (ii) LSGM-2520, (iii) LSGMF-251802, (iv) LSGMF-251604, and (v) LSGMF-251208. Non-perovskite phases, (○) $LaSrGa_3O_7$ and (□) $LaSrGaO_4$, are indicated.

Introduction of Sr^{2+} into the $LaGaO_3$ lattice increases the ABO_3 perovskite tolerance factor, which reduces the compressive stress on the BO_3 framework which is responsible for distorting the lattice from high to low symmetry [13]. However, if Sr^{2+} ions were added excessively the lattice would have a high concentration of oxygen vacancies which might cause association of oxygen vacancies or a complex defect structure. Losing symmetry, finally, induces the formation of secondary phases, such as $LaSrGa_3O_7$ and $LaSrGaO_4$, to release local stresses.

It seems that a structure-stabilizing effect of Fe would be related with the behavior of oxygen vacancies. Adding Fe^{3+} instead of Mg^{2+} would cause oxygen vacancies to be charge compensated in the lattice [8], and this may help to stabilize the "Sr-rich" structure. On the other hand, partial substitution of smaller Fe^{3+} ions in place of larger Mg^{2+} ions would cause an increase in tolerance factor. As Sr doping in $LaGaO_3$ already increases the tolerance factor over 0.96, which is the ideal tolerance factor for a perovskite structure because of cooperative rotations of the BO_3 octahedra [13], additional Fe

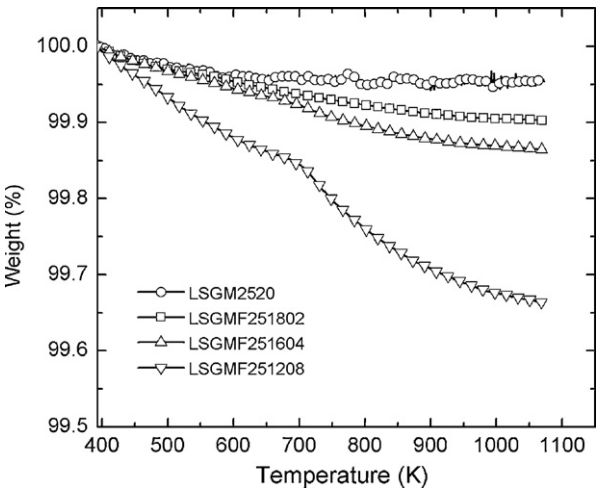

Fig. 2. Change in mass as a function of temperature for LSGM-2520, LSGMF-251802, LSGMF-251604, and LSGMF-251208.

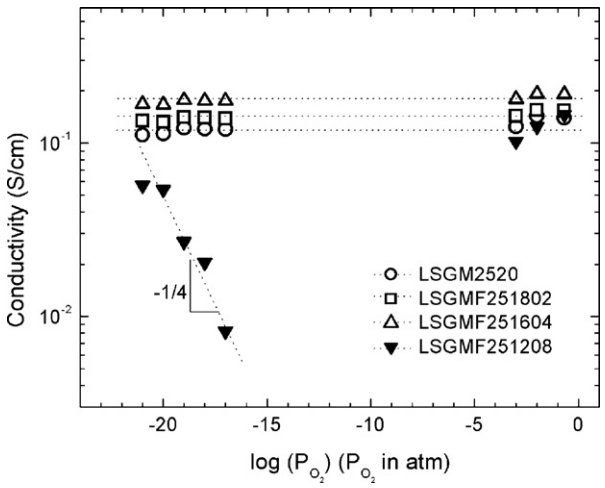

Fig. 3. Electrical conductivities as a function of oxygen partial pressure for LSGM-2520, LSGMF-251802, LSGMF-251604, and LSGMF-251208 at 1073 K.

doping could induce larger deviations from the symmetric structure because of mismatch in the equilibrium of A–O and B–O bond lengths. The reoccurrence of the secondary phases in LSGM doped with larger amounts of Fe (LSGMF-251208) could be explained by the increase in tolerance factor. Accordingly, optimal composition of Fe in the LSGM-2520 could be determined by the two competing effects of Fe doping on the stability of the highly symmetric perovskite phase.

Thermogravimetry analysis: Fig. 2 shows the relative weight change of LSGM-2520 and Fe-doped LSGM samples as a function of temperature under nitrogen. A weight loss at elevated temperatures was observed for all the compositions and seemed to be caused by a loss in lattice oxygen [6]. This behavior has been observed for other Fe- or Co-containing perovskite materials [14]. The weight loss of the LSGM-2520 specimen was the smallest of all the tested compositions and was less than 0.07 wt% of the original weight. The degree of weight change in Fe-doped LSGM increased with temperature and Fe doping level, which means that the presence of Fe ions is related with the loss of lattice oxygen.

The charges associated with oxygen vacancies need to be compensated by an oxidation of a variable-valence cation, or transition metal. The relation can be written as (using Kroger–Vink notation)

$$O_O^{\times} + 2Fe_{Mg}^{\bullet} \rightarrow \tfrac{1}{2}O_2 + V_O^{\bullet\bullet} + 2Fe_{Mg}^{\times} \quad (1)$$

Or the reduction in valence state of Fe cation from Fe^{3+} to Fe^{2+} could accommodate the charge associated with oxygen vacancy formation [6]. This is supported by the TGA results for LSGM-2520, which does not have a transition metal, showing almost negligible weight change with temperature. The effect of the oxygen vacancies created in Fe-doped LSGM on the conductivity is discussed further with the following conductivity data.

Electrical conductivity: Electrical conductivity of the undoped and Fe-doped LSGM samples was measured as a function of oxygen partial pressure at 1073 K as shown in Fig. 3. The conductivity of LSGM-2520, LSGMF-251802, and LSGMF-251604 was almost independent of the oxygen partial pressure at least from $P_{O_2} = 10^{-17}$ to 10^{-21} atm, which means that the electrical conductivity was primarily due to oxygen ionic conduction in this region. Although there seems to be a slight deviation from linearity in the electrical conductivity in the higher P_{O_2} region ($P_{O_2} = 10^{-3}$ to 1 atm) even for LSGM-2520, it is hard to tell decisively whether there is electron-hole conductivity or not. The conductivity of the three compositions, which showed independency on the oxygen partial pressure, increased in order of LSGM-2520 < LSGMF-251802 < LSGMF-251604, with a maximum conductivity of 0.17 S cm^{-1} (at 1073 K) for LSGMF-251604, which is almost the highest among the reported values.

On the other hand, the electrical conductivity of LSGMF-251208 decreased with increasing oxygen partial pressure in the low P_{O_2} region ($P_{O_2} = 10^{-17}$ to 10^{-21} atm). The dependency of the conductivity on the oxygen partial pressure was about −1/4, implying that electronic conduction was dominated by small polaron hopping of Fe^{2+}/Fe^{3+} in the low oxygen partial pressure range [15]. Even in the high P_{O_2} region ($P_{O_2} = 10^{-3}$ to 1 atm), there is a tendency for decreasing conductivity with decreasing P_{O_2}, implying that electron-hole may be the majority charge carriers in this range. Therefore, the substitution of Fe in the LSGM-2520 seems to be limited to less than 8 mol% of B-site occupation while maintaining the required solid electrolyte properties.

Ishihara et al. have reported that the ionic conductivities of LSGM, which has 20 mol% and less of Sr and Mg, were enhanced by substitution of a low amount (<10 mol% on the B-site) of transition metal, such as Fe or Co [8,16]. On the other hand, Stevenson et al. found that there was no increase in the ionic conductivity relative to the base LSGM composition when a small amount of Fe or Co was doped [6]. They attributed this apparent difference to the oxygen partial pressure difference in the conductivity measurement. According to the present results, ionic conductivity seemed to increase with a small amount of Fe doping.

The enhancement in ionic conductivity can be attributed to a change in concentration of charge carriers and the mobility of the oxide ions. The concentration of oxygen vacancies would be decreased by doping Fe^{3+} instead of Mg^{2+}. Therefore, we can assume that LSGM-2520 will have more oxygen vacancies than LSGMF-251604. In spite of the decreased amount of oxygen vacancies, the improved oxide ion conductivity seems to be explained by the improved mobility of the oxide ions. The origin of mobility enhancement by Fe doping would be the release of the local stress in the lattice which was induced by a high concentration of added Sr to the La position combined with the mismatch in ionic size [8]. This is because the ionic size of Fe^{3+} (64 pm) is intermediate between that of Ga^{3+} (62 pm) and Mg^{2+} (66 pm).

As discussed above, along with enhancing the phase stability, Fe doping of LSGM with as much as 4 mol% can cause a decrease in the concentration of oxygen vacancies compared to that of undoped LSGM. However, as long as there is no significant change in the lattice symmetry, mobility of oxide ions will be enhanced with Fe substitution for Mg to the extent of maintaining the undistorted structure, which turned out to be around 4–8 mol% in this system.

3.2. Crystal structure of LSGMF-251604

In view of the above results on phase stability and conductivity, we selected LSGMF-251604 as the most promising electrolyte composition and investigated its crystal structure as a function of temperature.

Neutron diffraction was used to obtain information on the atomic locations of LSGMF-251604 because it is more accurate in the determination of oxygen parameters in the presence of heavier metal atoms than X-ray diffraction [17]. $LaGaO_3$-based perovskite can have several different crystal structures depending on the temperature, i.e., cubic ($Pm\bar{3}m$), orthorhombic ($Pnma$), rhombohedral ($R\bar{3}c$), and monoclinic ($I2/a$) [17–19], which can be determined effectively by peak splitting [9,20]. Fig. 4(a) shows neutron diffraction patterns of LSGMF-251604 measured at various temperatures. An expanded view of the peaks in the 2θ range of 55–58° are shown in Fig. 4(b). These data show that there is no splitting in the parent

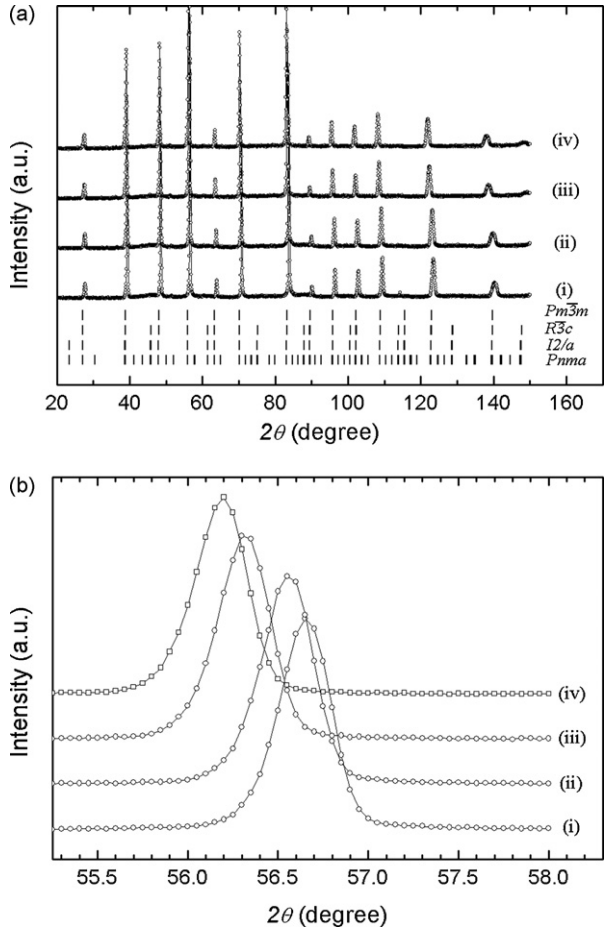

Fig. 4. Neutron diffraction patterns of LSGMF-251604 at the temperatures of (i) 298 K, (ii) 473 K, (iii) 773 K, and (iv) 973 K: (a) patterns in the range of $2\theta = 20–150°$ with tickmarks of cubic ($Pm\bar{3}m$), orthorhombic ($Pnma$), rhombohedral ($R\bar{3}c$), and monoclinic ($I2/a$); (b) an expanded patterns in the range of $2\theta = 55–58°$.

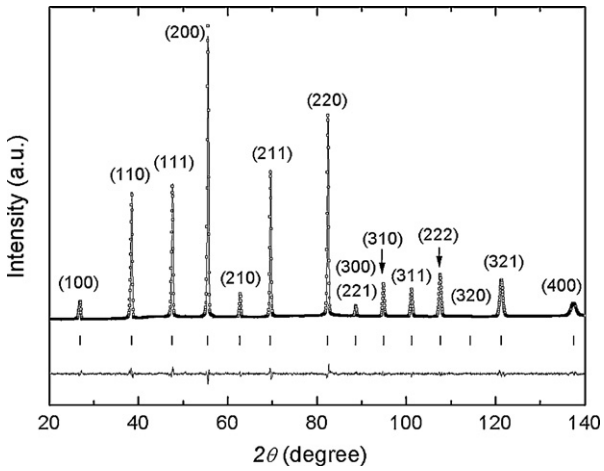

Fig. 5. The observed, calculated, and difference plots for the fit to neutron diffraction pattern of LSGMF-251604 after Rietveld refinement of the crystal structure at 973 K.

Table 1
Refined structural parameters for LSGMF-251604 at 298, 473, 773, and 973 K.

Parameters	LSGMF-251604 (cubic) $La_{0.75}Sr_{0.25}Ga_{0.8}Mg_{0.16}Fe_{0.04}O_{3-\delta}$[a]			
	298 K[b]	473 K[b]	773 K[b]	973 K[b]
a (Å)	3.9096(1)	3.9158(1)	3.9309(1)	3.9386(1)
V (Å^3)	59.760(2)	60.047(3)	60.742(3)	61.101(3)
Space group	$Pm\bar{3}m$	$Pm\bar{3}m$	$Pm\bar{3}m$	$Pm\bar{3}m$
R_e (%)	6.45	6.27	6.59	6.98
R_{wp} (%)	9.80	9.41	9.52	10.2
R_B (%)	2.08	1.79	1.48	1.64
χ^2	2.31	2.25	2.09	2.12

[a] Empirical formula.
[b] Temperature.

diffraction pattern with increasing temperature, which connotes no structural change up to 973 K. Comparing the diffraction patterns collected in the range of $0° < 2\theta < 159.95°$ to the positions of the four possible phases as shown in Fig. 4(a) indicates that the measured peaks correspond to those of the crystal having high symmetry and a space group $Pm\bar{3}m$ at all the temperatures.

For the Rietveld refinement, the site occupancy factors of La and Ga were fixed, except for O atoms, assuming that molar ratio of the each component would follow a stoichiometric composition. The observed and calculated diffraction patterns of LSGMF-251604 at 973 K are shown in Fig. 5, and the summary of the results was listed in Table 1. A $Pm\bar{3}m$ symmetry model for LSGMF-251604 gave a low R factor, a measurement of agreement between an observed peak and a calculated one. The lattice parameter of LSGMF-251604 is $a = 3.9096(1)$ Å for a cubic unit cell at room temperature. As temperature increases, the volume of the LSGMF-251604 unit cell increased. The site occupancy factor of oxygen atoms in LSGMF-251604 was approximately 2.75 at 973 K.

Electron diffraction was used to confirm the structural parameters of LSGMF-251604. Using the crystal structure data obtained from the Rietveld refinement, the expected electron diffraction pattern was calculated. The SAED pattern, as shown in Fig. 6(a), proves that the specimen was polycrystalline. The interplanar distances of (1 0 0) and (1 2 1) in LSGMF-251604 crystal, measured with referencing silicon as a standard, were 2.76 and 1.59 Å, respectively. The values are very close to those, 2.765 and 1.596 Å, measured with the simulated pattern (Fig. 6(b)), implying that cubic $Pm\bar{3}m$ symmetry is reasonable for the LSGMF-251604 composition.

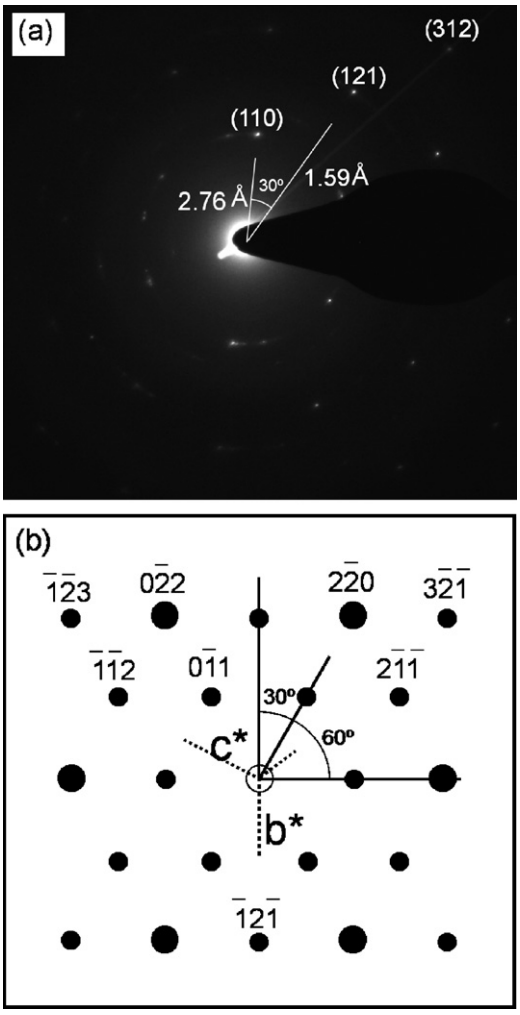

Fig. 6. (a) SAED pattern in zone axis [1 1 1] and (b) simulated pattern for LSGMF-251604. Interplanar distances measured from the simulated pattern are $d_{1\,1\,0}$ = 2.765 Å, $d_{1\,2\,1}$ = 1.596 Å, and $d_{3\,1\,2}$ = 1.045 Å.

4. Conclusion

The phase stability and electrical conductivity of 25 mol% Sr-doped and 20 mol% Mg-doped $LaGaO_3$ has been investigated as a function of amount of Fe dopant in B-sites. While increasing the amount of Fe to 4 mol%, secondary phases were eliminated and the electrical conductivity increased to 0.17 S cm^{-1} at 800 °C. Dependency of the conductivity on the oxygen partial pressure confirms that it is mainly ionic. Excess doping of Fe to 8 mol% caused phase instability and loss of ionic conduction.

According to a neutron and electron diffraction, 4 mol% Fe-doped LSGM-2520 has high symmetry, cubic $Pm\bar{3}m$. Additionally, no phase transition was detected at temperatures up to 973 K. LSGMF-251604 is expected to be a promising electrolyte composition for SOFC usable at intermediate temperatures.

References

[1] K. Huang, R.S. Tichy, J.B. Goodenough, J. Am. Ceram. Soc. 81 (1998) 2581.
[2] K. Kuroda, I. Hashimoto, K. Adachi, J. Akikusa, Y. Tamou, N. Komada, T. Ishihara, Y. Takita, Solid State Ionics 132 (2000) 199.
[3] T. Ishihara, H. Matsuda, M.A. Bustam, Y. Takita, Solid State Ionics 86–88 (1996) 197.
[4] J.W. Stevenson, T.R. Armstrong, L.R. Pederson, J. Li, C.A. Lewinsohn, S. Baskaran, Solid State Ionics 113–115 (1998) 571.
[5] T. Ishihara, H. Matsuda, Y. Takita, J. Am. Ceram. Soc. 116 (1994) 3801.
[6] J.W. Stevenson, K. Hasinska, N.L. Canfield, T.R. Armstrong, J. Electrochem. Soc. 147 (2000) 3213.
[7] T. Ishihara, T. Akbay, H. Furutani, Y. Takita, Solid State Ionics 113–115 (1998) 585–591.
[8] T. Ishihara, T. Shibayama, M. Honda, H. Nishiguchi, Y. Takita, J. Electrochem. Soc. 147 (2000) 1332.
[9] N. Trofimenko, H. Ullmann, Solid State Ionics 118 (1999) 215.
[10] T. Ishihara, H. Furutani, M. Honda, T. Yamada, T. Shibayama, T. Akbay, N. Sakai, H. Yokokawa, Y. Takita, Chem. Mater. 11 (1999) 2081.
[11] P.-N. Huang, A. Petric, J. Electrochem. Soc. 143 (1996) 1644.
[12] S. Li, B. Bergman, J. Eur. Ceram. Soc. 29 (2008) 1139.
[13] K. Huang, J.B. Goodenough, J. Alloys Compd. 303–304 (2000) 454.
[14] J.W. Stevenson, T.R. Armstrong, R.D. Carneim, L.R. Pederson, W.J. Weber, J. Electrochem. Soc. 143 (1996) 2722.
[15] C.C. Chen, M.M. Nasrallah, H.U. Anderson, J. Electrochem. Soc. 142 (1995) 491.
[16] T. Ishihara, T. Shibayama, M. Honda, H. Nishiguchi, Y. Takita, Chem. Commun. (1999) 1227.
[17] M. Lerch, H. Boysen, T. Hansend, J. Phys. Chem. Solids 62 (2001) 445.
[18] P.R. Slater, J.T.S. Irvine, T. Ishihara, Y. Takita, J. Solid State Electrochem. 139 (1998) 135.
[19] L. Vasylechko, V. Vashook, D. Savytskii, A. Senyshyn, R. Niewa, M. Knapp, H. Ullmann, M. Berkowski, A. Matkovskii, U. Bismayerg, J. Solid State Chem. 172 (2003) 396.
[20] F. Chen, M. Liu, J. Solid State Electrochem. 3 (1998) 7.